Imperial/TP/94-95/16
hep-ph/9502209
31^{st} January 1995

Thermalisation of Gauge Bosons in the Abelian Higgs Model

T.S.Evans* **& A.C.Pearson**†
Blackett Laboratory, Imperial College, Prince Consort Road,
London SW7 2BZ U.K.

Abstract

The thermalisation rate for long wavelength fluctuations of the gauge field in the abelian Higgs model is calculated from the imaginary part of the self energy. The calculation is performed for both the symmetric and symmetry broken phase of the theory.

1 Introduction

The study of gauge theories at high temperatures has found application in the description of a quark-gluon plasma in heavy ion collisions and for the physics of the early universe. In recent years, it has become apparent that conventional perturbation theory breaks down when considering energy scales much smaller than the temperature. In the case of hot QCD, this realisation led to the development of a resummation scheme based on hard thermal loops[1, 2].

Recently in a paper by Elmfors, Enqvist and Vilja [3], the method of hard thermal loops was applied to the electroweak theory in order to determine the thermalisation rate of fluctuations in the Higgs field. In this paper, we use the same methods to study the thermalisation rate of the gauge field in the abelian Higgs model. This is a first step towards the calculation of the thermalisation rate for a more realistic theory. The thermalisation rate may be used to determine the time at which the gauge bosons associated with a grand unified theory will 'freeze out' in an expanding universe. This may be of use in the subject of baryogenesis in the early universe.

*E-Mail: T.Evans@IC.AC.UK
†E-mail: A.Pearson@IC.AC.UK

In the present paper we calculate the thermalisation rate γ from the imaginary part of the temperature dependent Feynman self energy Σ via [4, 5]

$$\gamma = -\frac{\mathrm{Im}\Sigma(\omega,\mathbf{k})}{2\omega} \tag{1}$$

where ω is the energy of a given mode. We shall be calculating the thermalisation rate of large scale fluctuations (that is at zero 3-momentum). We use the real time formalism of thermal field theory[4, 5, 6, 7] since it is straightforward to extract the imaginary part of the self energy in this formalism [8].

The paper is organised as follows. In section 2 we give a brief overview of the abelian Higgs model and present the corrections to the propagators and vertices in the hard thermal loop approximation. In section 3 we use these results to calculate the thermalisation rate both above and below the critical temperature at which the phase transition occurs. Finally, we discuss the results in section 4.

2 The Abelian Higgs model

The abelian Higgs model consists of a complex scalar field minimally coupled to a $U(1)$ gauge field. It is described by the Lagrangian

$$\mathcal{L} = -\tfrac{1}{4}F^{\mu\nu}F_{\mu\nu} + (D^\mu\Phi)^*(D_\mu\Phi) - \rho^2\Phi^*\Phi - \tfrac{\lambda}{6}(\Phi^*\Phi)^2 \tag{2}$$

with covariant derivative $D^\mu = \partial^\mu - \imath eA^\mu$ and abelian field strength tensor $F^{\mu\nu} = \partial^\mu A^\nu - \partial^\nu A^\mu$. We choose $\rho^2 < 0$ so that spontaneous symmetry breaking occurs. Expanding Φ about its expectation value as

$$\Phi(x) = \frac{1}{\sqrt{2}}\Big(v + \phi(x) + \imath\chi(x)\Big)$$

we may rewrite Eqn.2 as $\mathcal{L} = \mathcal{L}_0 - V(A^\mu,\phi,\chi)$ where

$$\begin{aligned}\mathcal{L}_0 \;=\; & -\tfrac{1}{4}F^{\mu\nu}F_{\mu\nu} + \tfrac{1}{2}M^2A^\mu A_\mu \\ & +\tfrac{1}{2}\partial^\mu\phi\partial_\mu\phi - \tfrac{1}{2}m^2\phi^2 + \tfrac{1}{2}\partial_\mu\chi\partial^\mu\chi - M\partial_\mu\chi A^\mu\end{aligned} \tag{3}$$

and $V(A^\mu,\phi,\chi)$ is a potential term containing only cubic and quartic terms. $M = ev$ and $m^2 = \frac{1}{3}\lambda v^2$. We assume $\lambda \sim e^2$.

The gauge is chosen so as to simplify the calculation. That is we choose the gauge so as to both simplify the explicit form of the propagators used and also to reduce the number of diagrams contributing to hard thermal loops. To this end we choose to use the t'Hooft gauge (the renormalisable R_ζ gauge with $\zeta = 1$).

We do not use the covariant gauge as the propagators in this gauge must be resummed due to mixing between the photon and the unphysical goldstone mode. As shown in [9], this resummation leads to real time propagators that contain derivatives of Dirac delta

functions. Although there is in principle no problem with using such propagators, it is much simpler to use the renormalisable gauges which do not need this kind of resummation.

The t'Hooft gauge is then chosen as it enables us to reduce the number of diagrams contributing hard thermal loops. This is due to the particularly simple form of the photon propagator. The only disadvantage of this choice of gauge is that Fadeev-Popov ghosts must be included.

As a result of this choice of gauge, the following terms must be added to the lagrangian.

$$\mathcal{L}_{g.f.} = -\frac{1}{2}\Big(\partial_\mu A^\mu + M\chi\Big)^2 - \bar{c}\Big(\Box + M^2 + eM\phi\Big)c \tag{4}$$

where c is the ghost field. As a result of this choice of gauge, the Goldstone mode acquires a mass M equal to that of the gauge boson.

2.1 Leading order results

The leading order corrections in the hard thermal loop approximation are known in the case of the abelian higgs model[10, 11, 12, 13, 14, 15]. We shall not repeat these calculations but merely quote the results. At high temperatures, the vacuum expectation value(VEV) decreases from it's zero temperature value, reaching zero at the critical temperature T_C. The temperature dependant VEV v_β is given by

$$v_\beta^2 = v^2 - \frac{T^2}{2}\left(\frac{2}{3} + 3\frac{e^2}{\lambda}\right) \tag{5}$$

The masses of the scalar and ghost sectors of the theory, are affected only by the change in the VEV. That is the temperature dependant masses m_β and M_β are defined by

$$\begin{aligned} m_\beta^2 &= \frac{1}{3}\lambda v_\beta^2 \\ M_\beta &= e v_\beta \end{aligned} \tag{6}$$

However for the gauge boson there is a high temperature correction in addition to that due to the temperature dependant VEV. This additional contribution depends on the polarisation. That is there are three mass corrections corresponding to the spatially transverse and longitudinal polarisations and to the 4-vector longitudinal polarisation. These masses are given by [10]

$$\begin{aligned} \text{Transverse:} \quad \Pi_T(k_0,\mathbf{k}) &= M_\beta^2 + \frac{e^2T^2}{6}\left\{\frac{k_0^2}{\mathbf{k}^2} + \left(1 - \frac{k_0^2}{\mathbf{k}^2}\right)\frac{k_0}{2\mathbf{k}}\ln\left(\frac{k_0+|\mathbf{k}|}{k_0-|\mathbf{k}|}\right)\right\} \\ \text{Longitudinal:} \quad \Pi_L(k_0,\mathbf{k}) &= M_\beta^2 + \frac{e^2T^2}{3}\left(1 - \frac{k_0^2}{\mathbf{k}^2}\right)\left\{1 - \frac{k_0}{2|\mathbf{k}|}\ln\left(\frac{k_0+|\mathbf{k}|}{k_0-|\mathbf{k}|}\right)\right\} \\ \text{4-longitudinal:} \quad \Pi_4^2 &= M_\beta^2 \end{aligned} \tag{7}$$

There are no hard thermal loop corrections to the vertices [13, 15].

We shall be calculating the thermalisation rate at zero momentum. As such we define M_T to be the value of the self energy of the transverse and longitudinal modes in this limit.

$$M_T^2 = \Pi_T(k_0, \mathbf{0}) = \Pi_L(k_0, \mathbf{0}) = M_\beta^2 + \frac{e^2T^2}{9} \tag{8}$$

Above the critical temperature, the symmetry is restored. There is now no distinction between the higgs and goldstone fields. The masses for the particles are now

$$\text{Higgs/Goldstone:} \quad m^2 = \tfrac{1}{12}(T^2 - T_C^2)\{\tfrac{2}{3}\lambda + 3e^2\}$$

$$\text{Photon:} \quad \text{As in Eqns.7-8 but with } M_\beta = 0 \tag{9}$$

3 Calculation of the thermalisation rate

To calculate the thermalisation rate we need the imaginary part of the self-energy[16]. In the real time formalism, the imaginary part of the Feynman self energy is most easily calculated from the 1-2 component of the self energy via the relation [8, 4]

$$\mathrm{Im}\Sigma = -\frac{e^{-\frac{\beta|k_0|}{2}}}{2n(|k_0|)}\mathrm{Im}\Sigma_{12} \tag{10}$$

where $n(X)$ is the Bose-Einstein distribution. We are working in the symmetric version of the real time formalism (that is $\sigma = \frac{1}{2}$ in the notation of Landsman and van Weert [4]).

3.1 Resummed propagators

To proceed with the calculation we need the explicit form for the 1-2 component of the resummed propagators. For the scalar and ghost sector of the theory, this is easy due to the simple form of the hard thermal loop mass correction. However care must be taken with the photon propagator due to the complicated momentum dependance of the self energies. The 1-2 propagators for the higgs and goldstone modes are given by

$$\text{Higgs:} \quad \imath\Delta_{12}^H(k) \;= 2\pi e^{\frac{\beta|k_0|}{2}} n(|k_0|)\delta(k^2 - m_\beta^2) \tag{11}$$

$$\text{Goldstone:} \quad \imath\Delta_{12}^G(k) \;= 2\pi e^{\frac{\beta|k_0|}{2}} n(|k_0|)\delta(k^2 - M_\beta^2) \tag{12}$$

We must take care with the photon propagator since for $k_0^2 < \mathbf{k}^2$ the self energies of the transverse and longitudinal modes acquire an imaginary contribution. By dividing the propagator up into it's three polarisations we can treat each case separately.

$$\imath\Delta_{12}^{\mu\nu}(k) = P_T^{\mu\nu}\imath\Delta_{12}^T(k) + P_L^{\mu\nu}\imath\Delta_{12}^L + \frac{k^\mu k^\nu}{k^2}\imath\Delta_{12}^4(k) \tag{13}$$

where $P_T^{\mu\nu}$ and $P_L^{\mu\nu}$ are the transverse and longitudinal projection operators. In the rest frame of the heat bath they are given by

$$\begin{aligned}
P_T^{00}(k) &= P_T^{0i}(k) = P_T^{i0}(k) = 0 \\
P_T^{ij}(k) &= -\Big(\delta^{ij} - \frac{k^i k^j}{\mathbf{k}^2}\Big) \\
P_L^{\mu\nu}(k) &= \Big(g^{\mu\nu} - \frac{k^\mu k^\nu}{k^2}\Big) - P_T^{\mu\nu}(k)
\end{aligned} \tag{14}$$

From this we find that $\Delta_{12}^4(k) = -\Delta_{12}^G(k)$. To calculate Δ_{12}^T and Δ_{12}^L we use the relation

$$\Delta_{12} = e^{\frac{\beta|k_0|}{2}} n(|k_0|)\Big(\Delta_F - \Delta_F^*\Big) \tag{15}$$

where in Δ_F we replace k_0 by $k_0 + \imath\varepsilon$ ($k_0 - \imath\varepsilon$) when k_0 is greater than (less than) zero. Using this we find that the transverse propagator is given by

$$\begin{aligned}
\imath\Delta_{12}^T(k_0,\mathbf{k}) &= -2\pi e^{\frac{\beta|k_0|}{2}} n(|k_0|)\delta(k^2 - \Pi_T(k_0,\mathbf{k})) & k_0^2 > \mathbf{k}^2 \\
&= -2\pi e^{\frac{\beta|k_0|}{2}} n(|k_0|)\frac{2M_{TC}^2(k_0,\mathbf{k})}{\Big(k^2 - \mathrm{Re}(\Pi_T(k_0,\mathbf{k}))\Big)^2 + M_{TC}^4(k_0,\mathbf{k})} & k_0^2 < \mathbf{k}^2
\end{aligned} \tag{16}$$

where Π_T is given by Eqn.7 and M_{TC} is

$$M_{TC}^2(k_0,\mathbf{k}) = \pi\frac{e^2T^2}{12}\frac{|k_0|}{|\mathbf{k}|}\Big(1 - \frac{k_0^2}{\mathbf{k}^2}\Big) \tag{17}$$

Similarly, the longitudinal propagator is given by

$$\begin{aligned}
\imath\Delta_{12}^L(k_0,\mathbf{k}) &= -2\pi e^{\frac{\beta|k_0|}{2}} n(|k_0|)\delta(k^2 - \Pi_L(k_0,\mathbf{k})) & k_0^2 > \mathbf{k}^2 \\
&= -2\pi e^{\frac{\beta|k_0|}{2}} n(|k_0|)\frac{2M_{LC}^2(k_0,\mathbf{k})}{\Big(k^2 - \mathrm{Re}(\Pi_L(k_0,\mathbf{k}))\Big)^2 + M_{LC}^4(k_0,\mathbf{k})} & k_0^2 < \mathbf{k}^2
\end{aligned} \tag{18}$$

with Π_L given by Eqn.7 and M_{LC} is

$$M_{LC}^2(k_0,\mathbf{k}) = -\pi\frac{e^2T^2}{6}\frac{|k_0|}{|\mathbf{k}|}\Big(1 - \frac{k_0^2}{\mathbf{k}^2}\Big) \tag{19}$$

3.2 The calculation

There are only two diagrams contributing to Σ_{12}. They are shown in Fig.1. From these diagrams, we find that $\Sigma_{12}^{\mu\nu}$ is given by

$$\Sigma_{12}^{\mu\nu}(p_0,\mathbf{p}) = -\imath e^2\int d^4k\Big\{4M_\beta^2\imath\Delta_{12}^{\mu\nu}(k) + (p-2k)^\mu(p-2k)^\nu\imath\Delta_{12}^G(k)\Big\}\imath\Delta_{12}^H(p-k) \tag{20}$$

$-\imath\Sigma_{12}^{\mu\nu}(p) =$ 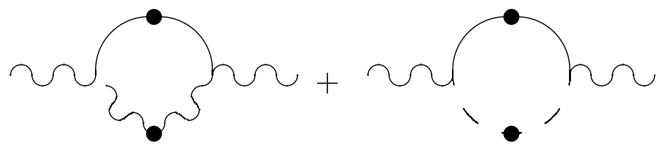

Figure 1: Feynman diagrams contributing to $\mathrm{Im}\Sigma_{12}^{\mu\nu}$ (Dot denotes hard thermal loop corrected propagator)

Using this we may now calculate the imaginary part of the transverse and longitudinal self-energies.

$$
\begin{aligned}
\mathrm{Im}\Sigma_{12}^{T}(p_0,\mathbf{p}) &= \frac{1}{2}P_{\mu\nu}^{T}(p)\mathrm{Im}\Sigma_{12}^{\mu\nu}(p_0,\mathbf{p}) \\
&= -2e^2M_\beta^2P_{\mu\nu}^{T}(p)\int\frac{d^4k}{(2\pi)^4}\imath\Delta_{12}^{H}(p-k)\Big\{P_T^{\mu\nu}(k)\imath\Delta_{12}^{T}(k)+P_L^{\mu\nu}(k)\imath\Delta_{12}^{L}(k)\Big\} \\
&\qquad -\frac{e^2}{2}\int\frac{d^4k}{(2\pi)^4}\imath\Delta_{12}^{H}(p-k)\imath\Delta_{12}^{G}(k). \\
&\qquad .P_{\mu\nu}^{T}(p)\Big\{(p-2k)^\mu(p-2k)^\nu-4M_\beta^2\frac{k^\mu k^\nu}{k^2}\Big\}
\end{aligned} \tag{21}
$$

We have divided up the integral in Eqn.21 into two sections. The first term contains the contribution from the physical modes of the photon propagator. The second term contains the contribution from the unphysical modes of the photon propagator and the contribution from the Goldstone propagator. Evaluating the second term in Eqn.21 (which we shall label as Σ_{12}^{U}), we find

$$
\Sigma_{12}^{U} = 2e^2\int\frac{d^4k}{(2\pi)^4}\imath\Delta_{12}^{H}(p-k)\imath\Delta_{12}^{G}(k)\frac{(k^2-M_\beta^2)}{k^2}\Big(\mathbf{k^2}-\frac{(\mathbf{p.k})^{\mathbf{2}}}{\mathbf{p^2}}\Big) = 0 \tag{22}
$$

due to the Dirac delta function in $\Delta_{12}^{G}(k)$. We therefore find that the only contribution to $\mathrm{Im}\Sigma_T$ comes from the physical modes of the theory. This suggests that our calculation is gauge invariant.

$$
\mathrm{Im}\Sigma_T = e^2M_\beta^2\frac{e^{\frac{\beta|p_0|}{2}}}{n(|p_0|)}\int\frac{d^4k}{(2\pi)^4}\imath\Delta_{12}^{H}(p-k)P_T^{\mu\nu}(p)\Big\{P_{\mu\nu}^{T}(k)\imath\Delta_{12}^{T}(k)+P_{\mu\nu}^{L}(k)\imath\Delta_{12}^{L}(k)\Big\} \tag{23}
$$

Similarly, when calculating $\mathrm{Im}\Sigma_L$, the unphysical contributions cancel out.

We now evaluate Eqn.23 at $p_0 = M_T, \mathbf{p} = \mathbf{0}$. The integration splits up into two regions corresponding to the two regions over which Δ_{12}^{T} and Δ_{12}^{L} are defined (see Eqns.16-19). That is we split up the integral into the regions $k^2 > 0$ and $k^2 < 0$. There is no contribution from the region $k^2 > 0$ since at zero momentum we cannot simultaneously satisfy both Dirac delta functions in Eqn.23.

The region $k^2 < 0$ does contribute. Performing all but the final momentum integration we find

$$
\begin{aligned}
\mathrm{Im}\Sigma_T &= -\frac{e^2 M_\beta^2}{3\pi^2}\int_{k>|M_T-\omega|} dk \frac{k^2}{\omega}\frac{n(|M_T-\omega|)n(\omega)}{n(M_T)} e^{\frac{\beta}{2}(|M_T-\omega|+\omega-M_T)}. \\
&\Big[\frac{2M_{TC}(M_T-\omega,k)}{\Big((M_T-\omega)^2-k^2-\Pi_T(M_T-\omega,k)\Big)^2+M_{TC}^4(M_T-\omega,k)} \\
&+\frac{(M_T-\omega)^2}{(M_T-\omega)^2-k^2}\frac{M_{LC}(M_T-\omega,k)}{\Big((M_T-\omega)^2-k^2-\Pi_L(M_T-\omega,k)\Big)^2+M_{LC}^4(M_T-\omega,k)}\Big]
\end{aligned}
\tag{24}
$$

Similarly $\mathrm{Im}\Sigma_L$ may be evaluated. At zero momentum we find $\mathrm{Im}\Sigma_T = \mathrm{Im}\Sigma_L$. This is to be expected since at zero momentum one cannot distinguish between transverse and longitudinal polarisations.

We must now consider the high temperature limit. Examining the temperature dependant terms from Eqn.24, and using the Mellin transformation[4, 17] to extract the high temperature behaviour we find

$$
\frac{n(|M_T-\omega|)n(\omega)}{n(M_T)} e^{\frac{\beta}{2}(|M_T-\omega|+\omega-M_T)} = \begin{cases} 1+n(\omega)+n(M_T-\omega) & M_T>\omega \\ n(\omega-M_T)-n(\omega) & M_T<\omega \end{cases} \tag{25}
$$

$$
\sim \frac{M_T T}{\omega|M_T-\omega|} \tag{26}
$$

We therefore find that to $O(e^2T)$, the thermalisation rate is given by

$$
\gamma(\mathbf{p}=0) = \frac{e^2T}{24\pi}.A(\tfrac{T}{T_C},\tfrac{\lambda}{e^2}) \tag{27}
$$

where $A(\frac{T}{T_C},\frac{\lambda}{e^2})$ is a dimensionless function of the ratio $\frac{\lambda}{e^2}$ and the ratio of the temperature to the critical temperature. We have chosen the factor of 24π in Eqn.27 so as to compare the result with the thermalisation rate above the critical temperature (See section 3.3).

$$
\begin{aligned}
A(\frac{T}{T_C},\frac{\lambda}{e^2}) &= \int_{\bar{k}>|\bar{M}_T-\bar{\omega}|} d\bar{k}\frac{2\bar{M}_\beta^2}{3\bar{\omega}^2\bar{k}}. \\
&.\Big[\frac{\bar{k}^2-(\bar{M}_T-\bar{\omega})^2}{\Big((\bar{M}_T-\bar{\omega})^2-\bar{k}^2-\bar{\Pi}_T(\bar{M}_T-\bar{\omega},\bar{k})\Big)^2+\bar{M}_{TC}^4(\bar{M}_T-\bar{\omega},\bar{k})} \\
&+\frac{(\bar{M}_T-\bar{\omega})^2}{\Big((\bar{M}_T-\bar{\omega})^2-\bar{k}^2-\bar{\Pi}_L(\bar{M}_T-\bar{\omega},\bar{k})\Big)^2+\bar{M}_{LC}^4(\bar{M}_T-\bar{\omega},\bar{k})}\Big]
\end{aligned}
\tag{28}
$$

where the overline denotes that the variable has been scaled by a factor of eT. That is $\bar{k} = \frac{k}{eT}$. Note that $A(\frac{T}{T_C},\frac{\lambda}{e^2})$ is positive definite.

This expression depends on the validity of the hard thermal loop approximation. We are assuming that all the masses are smaller than the temperature by at least one factor of the coupling constant e. That is we should only trust the results for $\frac{v_\beta}{T} \leq 1$. We should also be careful that the constant $A(\frac{T}{T_C}, \frac{\lambda}{e^2}) \geq e$. In addition to this we must also be sure that we do not vary the value of $\frac{\lambda}{e^2}$ so as to invalidate our assumption that $\lambda \sim e^2$. The temperature dependance of $A(\frac{T}{T_C}, \frac{\lambda}{e^2})$ is shown in Fig.2 for a range of values of $\frac{\lambda}{e^2}$. It can be seen that near the critical temperature $A(\frac{T}{T_C}, \frac{\lambda}{e^2}) \sim 1$. However as the temperature decreases, $A(\frac{T}{T_C}, \frac{\lambda}{e^2})$ becomes smaller. This is due to the increasing size of M_β reducing the effect of Landau damping.

One might expect that since $A(\frac{T}{T_C}, \frac{\lambda}{e^2}) \propto M_\beta^2$, we should expect that $A(\frac{T}{T_C}, \frac{\lambda}{e^2})$ vanishes at the critical temperature. However, this is not the case. In Fig.3 we show the contribution to $A(\frac{T}{T_C}, \frac{\lambda}{e^2})$ from the two terms in Eqn.28. These correspond to the contributions from the transverse and longitudinal parts of the photon propagator. It can be seen that near the critical temperature the longitudinal contribution dominates. This is due to the behaviour of Π_T and Π_L near the light cone. As we approach the critical temperature, Π_L becomes small around the light cone and can compensate for the smallness of M_β in the integrand of Eqn.28. However, Π_T does not vanish and so the contribution to $A(\frac{T}{T_C}, \frac{\lambda}{e^2})$ from the first term in Eqn.28 vanishes as we approach the critical temperature.

3.3 Above the critical temperature

In the symmetric phase, only the second Feynman diagram in Fig.1 contributes to Σ_{12}. From this we find that the imaginary part of the self energy at zero momentum is given by

$$\mathrm{Im}\Sigma_T(p_0, \mathbf{p}) = -e^2 \frac{e^{\frac{\beta|p_0|}{2}}}{2n(|p_0|)} \int \frac{d^4k}{(2\pi)^4} P_T^{\mu\nu}(p)[p-2k]_\mu [p-2k]_\nu \imath\Delta_{12}^H(p-k)\imath\Delta_{12}^G(k) \tag{29}$$

Evaluating this we find that the thermalisation rate at zero momentum above the critical temperature is given by

$$\gamma(\mathbf{p}=0) = \frac{e^2T}{24\pi}\left(1 - \frac{4m^2}{M_T^2}\right)^{\frac{3}{2}} \qquad M_T > 2m \tag{30}$$

where $M_T = \frac{eT}{3}$ is the value of the transverse or longitudinal self energy at zero momentum and m is defined by Eqn.9. For $M_T > 2m$, this diagram does not contribute to the imaginary part of the self energy and the thermalisation rate is of a higher order in the perturbation expansion associated with hard thermal loops. Solving the equation $M_T = 2m$ we find that Eqn.30 is valid in the temperature region

$$1 \leq \frac{T}{T_C} \leq \sqrt{\frac{2\lambda + 9e^2}{2\lambda + 8e^2}} \tag{31}$$

It should be noted that the value of the thermalisation rate at the critical temperature is independent of whether we approach the critical temperature from above or below. The decay rate as a function of temperature is shown in Fig.4. This result is consistent with the thermalisation rate for scalar electrodynamics [13].

4 Conclusions

We have managed to calculate the thermalisation rate at zero momentum for the gauge boson in the abelian Higgs model. The next step is to consider extending this work to a more realistic theory that contains fermions and utilises a larger gauge symmetry. While studying such a theory is more involved, there are in principle no additional problems in calculating the thermalisation rate.

At the order to which we work a second order phase transition is indicated. However near the phase transition v_β is small and higher order corrections become important. The quantitative results may change but more importantly the qualitative picture may change and the theory may have a first order phase transition. However we may trust our results away from the critical temperature.

References

[1] R.D.Pisarski, Physica **A158** 146 (1989), E.Braaten and R.D.Pisarski, Nucl. Phys. **B337**, 569 (1990).

[2] E.Braaten and R.D.Pisarski, Phys. Rev. **D42** R2156 (1990).

[3] P.Elmfors, K.Enqvist, and I.Vilja, Nucl. Phys. **B412** 459 (1994).

[4] N.P. Landsman and Ch.G. van Weert, Phys.Rep.**145** (1987) 141.

[5] J.I. Kapusta, *Finite temperature Field Theory* (Cambridge University Press, Cambridge, 1989).

[6] A.J. Niemi and G.W. Semenoff, Ann. Phys. (NY) **152** (1984) 105; Nucl. Phys. **B230** (1984) 181.

[7] R.J.Rivers, Path Integral Methods in Quantum Field. Theory (Cambridge University Press, Cambridge, 1987).

[8] Y.Fujimoto, M.Morikawa, and M.Sasaki, Phys. Rev. **D33** 590 (1986).

[9] T.S.Evans and A.C.Pearson, Z. Phys. C **29** 123 (1995).

[10] A.V. Smilga, Phys. Lett. **B**222 462 (1989)

[11] Y. Ueda, Phys.Rev. **D**23, 1383 (1981).

[12] P.Arnold, E. Braaten, and S. Vokos, Phys. Rev. **D46** 3576 (1992).

[13] U.Kraemmer, A.K.Rebhan, and H.Schulz, Preprint DESY 94-034, ITP-UH-01/94, hep-ph/9403301.

[14] A.K. Rebhan, Preprint hep-ph/9404292.

[15] J.Frenkel and J.C.Taylor, Nucl. Phys. **B334** 199 (1990).

[16] H.A.Weldon, Phys. Rev. **D28** 2007 (1983).

[17] G.Cheetham, E. Copeland,T.S. Evans, and R.J. Rivers, Phys. Rev. **D47** 5316 (1993).

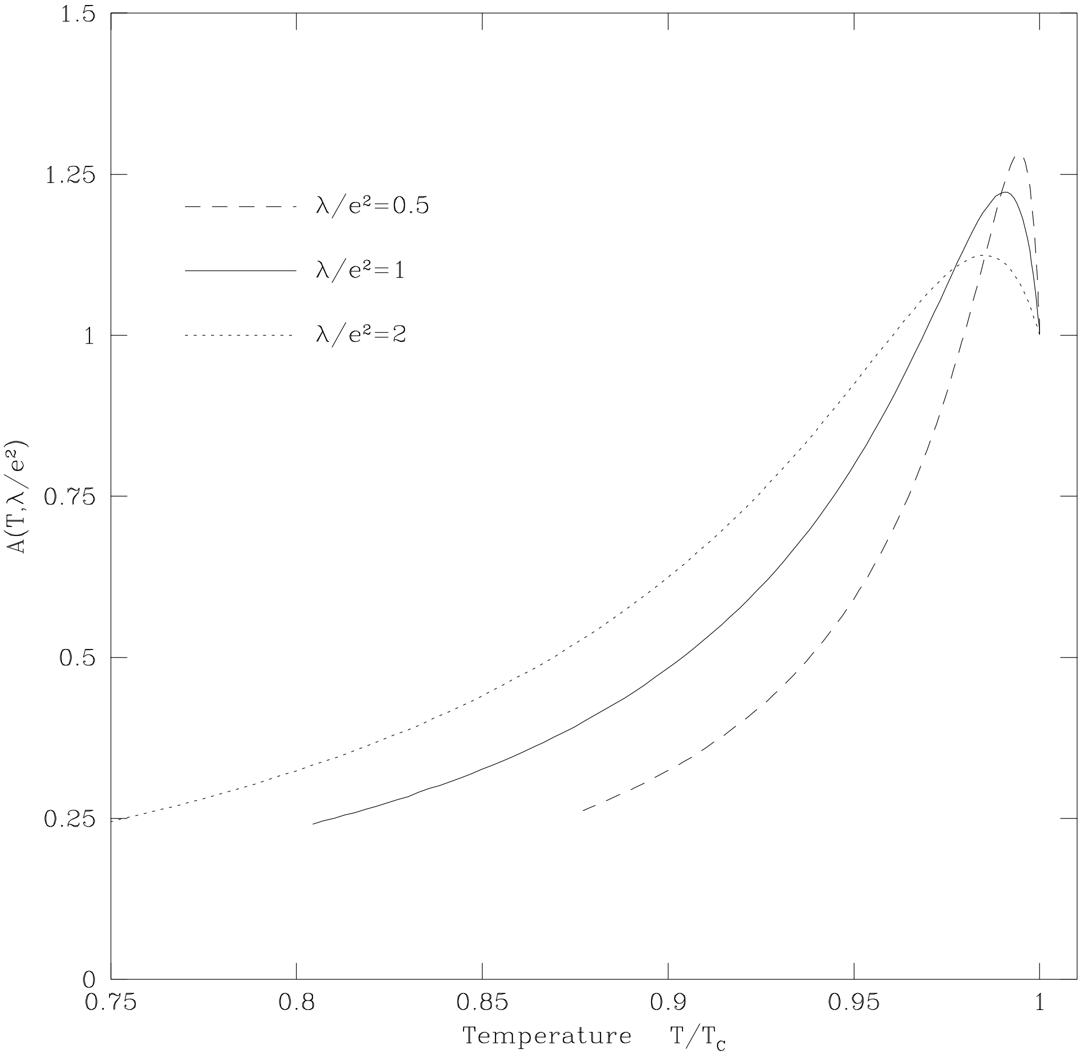

Figure 2: Temperature dependance of the constant $A(T, \frac{\lambda}{e^2})$

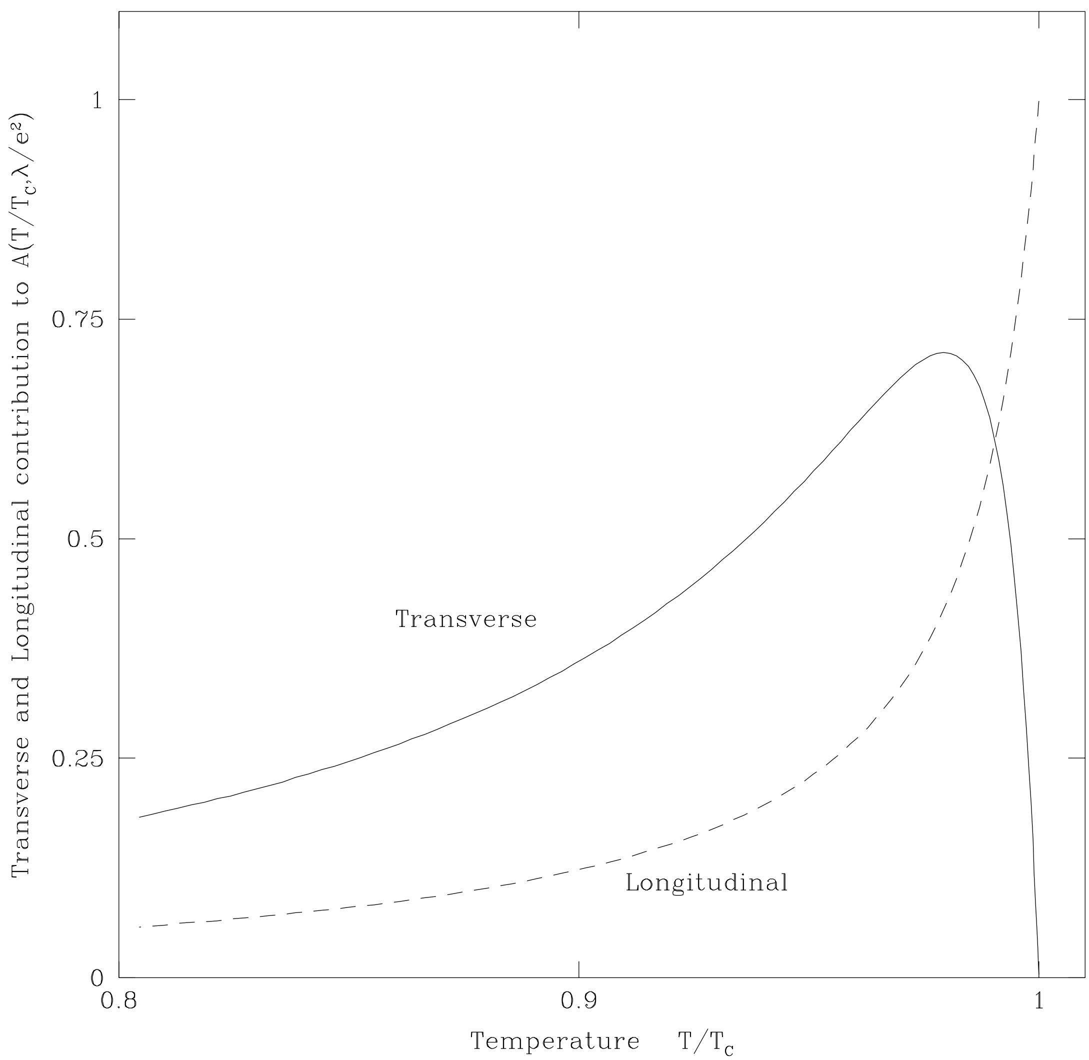

Figure 3: Contribution to $A(\frac{T}{T_C}, \frac{\lambda}{e^2})$ from the transverse and longitudinal parts of Eqn.28

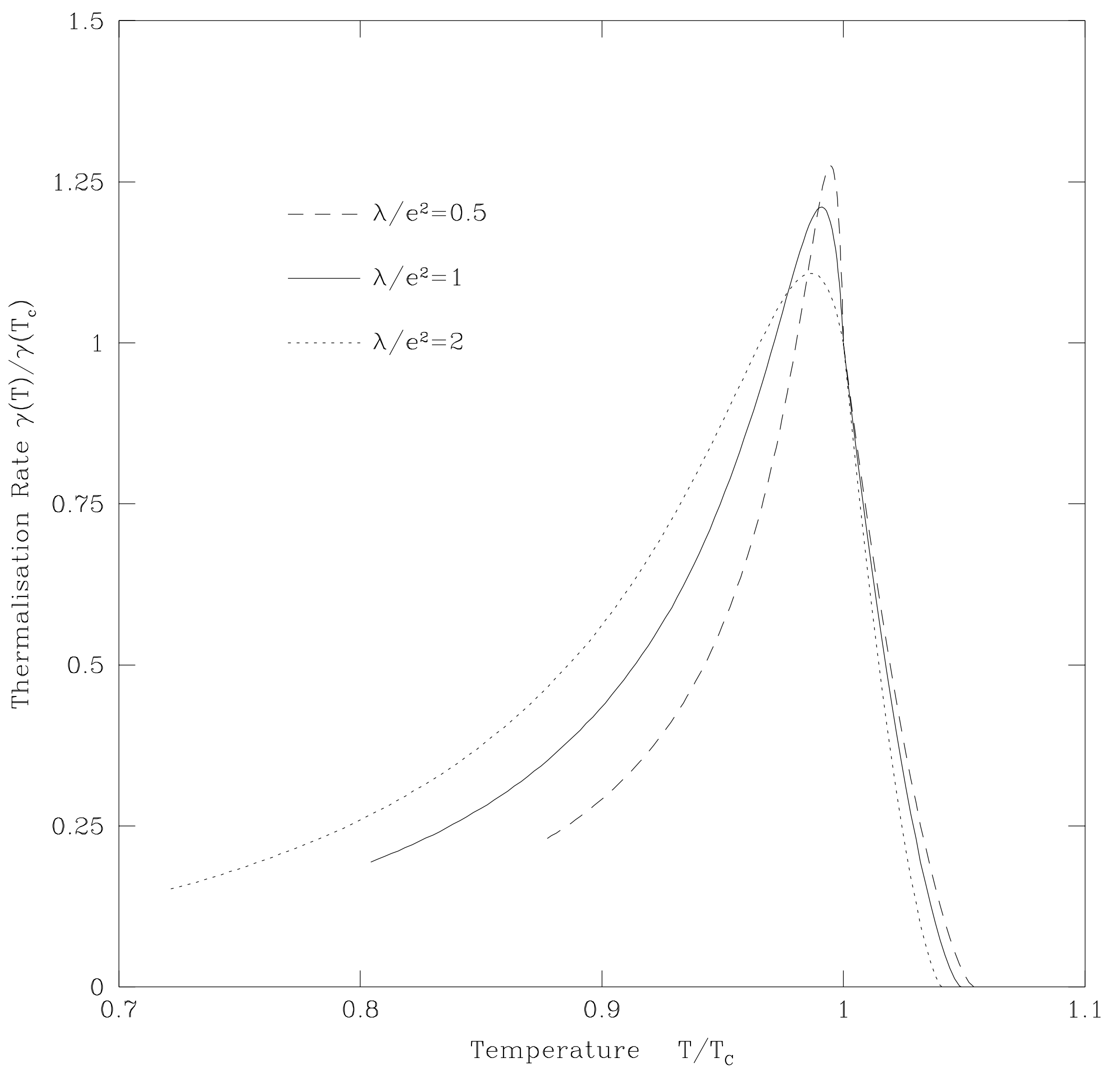

Figure 4: Plot of thermalisation rate versus temperature